

# A Monte Carlo study of jet fragmentation functions in PbPb and pp collisions at $\sqrt{s} = 2.76$ TeV

Redamy Pérez-Ramos<sup>1 2 3 4 5</sup>, Thorsten Renk<sup>6 7 8</sup>

The parton-to-hadron fragmentation functions (FFs) obtained from the YAJEM and PYTHIA6 Monte Carlo event generators, are studied for jets produced in a strongly-interacting medium and in the QCD “vacuum” respectively. The medium modifications are studied with the YAJEM code in two different scenarios by (i) accounting for the medium induced virtuality  $\Delta Q^2$  transferred to the leading parton from the medium, and (ii) by altering the infrared sector in the Borghini-Wiedemann approach. The results of our simulations are compared to experimental jet data measured by the CMS experiment in PbPb and pp collisions at a center-of-mass energy of 2.76 TeV. Though both scenarios qualitatively describe the shape and main physical features of the FFs, the ratios are in much better agreement with the first scenario. Results are presented for the Monte Carlo FFs obtained for different parton flavours (quark and gluon) and accounting exactly, or not, for the experimental jet reconstruction biases.

---

<sup>1</sup> Department of Physics, P.O. Box 35, FI-40014 University of Jyväskylä, Jyväskylä, Finland

<sup>2</sup> Sorbonne Université, UPMC Univ Paris 06, UMR 7589, LPTHE, F-75005, Paris, France

<sup>3</sup> CNRS, UMR 7589, LPTHE, F-75005, Paris, France

<sup>4</sup> Postal address: LPTHE tour 13-14, 4<sup>ème</sup> étage, UPMC Univ Paris 06, BP 126, 4 place Jussieu, F-75252 Paris Cedex 05 (France)

<sup>5</sup> e-mail: redamy.r.perez-ramos@jyu.fi, perez@lpthe.jussieu.fr

<sup>6</sup> Department of Physics, P.O. Box 35, FI-40014 University of Jyväskylä, Jyväskylä, Finland

<sup>7</sup> Helsinki Institute of Physics, P.O. Box 64, FI-00014 University of Helsinki, Helsinki, Finland

<sup>8</sup> e-mail: thorsten.i.renk@jyu.fi, trenk@phy.duke.edu

# 1 Introduction

Experiments at the Relativistic Heavy Ion Collider (RHIC) and Large Hadron Collider (LHC) have observed the formation of a Quark-Gluon Plasma (QGP) in AuAu and PbPb collisions respectively. Highly virtual quarks and gluons (generically called partons) lose energy as they traverse the QGP, resulting in the suppression of high transverse momentum leading hadrons [1–4] and jets [5, 6] as well as in the modification of jet fragmentation functions and jet shapes [7–9], observed in central heavy-ion collisions.

In the vacuum, the production of highly virtual partons issuing from a hard scattering of two partons from the incoming protons results in a spray of collimated hadrons observed in the final-state of the collision. The evolution of successive splittings  $q(\bar{q}) \rightarrow q(\bar{q})g$ ,  $g \rightarrow gg$  and  $g \rightarrow q\bar{q}$  ( $q$ ,  $\bar{q}$  and  $g$  label quark, antiquark and gluon respectively) inside the parton shower prior to hadronization can be computed analytically from perturbative QCD calculations resumming collinear and infrared divergences [10] or, alternatively, in terms of Monte Carlo (MC) formulations of the parton branching process such as the PYSHOW algorithm implemented in PYTHIA [11, 12]. In nucleus-nucleus (A-A) collisions, partons produced in the hard scatterings of two partons from the nuclei propagate through the hot/dense QCD medium also produced in such collisions and their branching pattern is changed by interacting with the color charges of the deconfined QGP [13]. As a consequence, additional medium-induced soft gluon radiation is produced in A-A collisions, which leads for instance to the suppression of high- $p_T$  hadroproduction [14–16] and a plethora of other jet modifications (see e.g. [17]). In the past few years, MC codes for in-medium shower simulations developed for hadronic collisions have also become available [18–22]. They have been based on the success of MC shower simulations in the vacuum such as PYTHIA and HERWIG [23].

The parton-to-hadron jet fragmentation functions (FFs),  $\frac{dN}{d\xi} \equiv zD_{i \rightarrow h}(z, Q)$  with  $\xi = \ln(1/z)$ , encode the probability that a parton  $i$  fragments into a hadron  $h$  carrying a fraction  $z$  of the parent parton’s momentum. In this paper, we compute the medium-modified FFs and the FF ratio of the fragment yield with YAJEM, where the medium itself is described by a 3-d hydrodynamical evolution [19, 20]. We compare our results with recent PbPb and pp CMS data collected at center-of-mass energy 2.76 TeV [9]. In the first scenario of the YAJEM code, it is mainly assumed that the cascade of branching partons traverses a medium which, consistently with standard radiative loss pictures, is characterized by a local transport coefficient  $\hat{q}$  which measures the virtuality per unit length transferred from the medium to the leading parton. Hence, the virtuality of the leading parton is increased by the integrated amount “ $\Delta Q^2$ ” which opens up the phase space and leads to a softer shower. The second scenario is based on the Borghini-Wiedemann (BW) model [24], where the singular part of the branching kernels in the medium is enhanced by a factor  $1 + f_{\text{med}}$ , such that  $P_{a \rightarrow bc} = (1 + f_{\text{med}})/z + \mathcal{O}(1)$ , where  $a \rightarrow bc$  describes the possible QCD parton branchings, i.e.  $q(\bar{q}) \rightarrow q(\bar{q})g$  and  $g \rightarrow gg$  with  $g \rightarrow q\bar{q}$  unchanged. In this case, the softening of the shower is described by the larger amount of medium-induced soft gluons ( $f_{\text{med}} > 0$ ) as compared to the vacuum ( $f_{\text{med}} = 0$ ). In both scenarios, the final parton-to-hadron transition takes place in the vacuum, using the Lund model [25], for hadronization scales below  $Q_0 = 1$  GeV.

For the purpose of a realistic comparison of YAJEM and PYTHIA6 with the CMS data, the FF analysis is carried out by following the CMS analysis closely. Jets are reconstructed with the anti- $k_t$  algorithm [26, 27] with a resolution parameter  $R = 0.3$ . The clustering analysis is limited to charged particles with  $p_t > 1$  GeV inside the jet cone where  $P_T \geq 100, 120, 150$  GeV are required for jets (i.e.  $P_T$  stands for the jet

transverse momentum inside the jet cone after reconstruction) in the jet  $P_T$  ranges  $100 \leq P_T(\text{GeV}) \leq 120$ ,  $120 \leq P_T(\text{GeV}) \leq 150$ ,  $150 \leq P_T(\text{GeV}) \leq 300$  and  $100 \leq P_T(\text{GeV}) \leq 300$  reported by the CMS collaboration [9]. The condition  $p_t > 1$  GeV facilitates the experimental jet reconstruction (as it removes a very large underlying-event background) but can potentially bias the jet FF analysis. In order to illustrate the role of the bias caused by the jet-finding procedure, we compare the biased FFs (i.e. provided the CMS jet-finding conditions are fulfilled) with the unbiased FFs (i.e. the ones obtained by analyzing all jets, including the ones found close to their nominal energy) for both PbPb and pp CMS data.

## 2 Comparison with YAJEM and QGP hydrodynamics

In the vacuum, the PYSHOW algorithm [11, 12] is a well-tested numerical implementation of QCD shower simulations. YAJEM is based on the PYSHOW algorithm, to which it reduces in the limit of no medium effects. It simulates the evolution of a QCD shower as an iterated series of splittings of a parent into two offspring partons  $a \rightarrow bc$  where the energy of the offspring are obtained as  $E_b = zE_a$  and  $E_c = (1 - z)E_a$  and the virtuality of parents and offspring is ordered as  $Q_a \gg Q_b, Q_c$ . In the explicit kinematics of the MC shower, the singularities at  $z \rightarrow 0$  or  $z \rightarrow 1$  lie outside of the accessible phase space and no  $[\dots]_+$  regularization procedure is needed. The decreasing hard virtuality scale of partons provides, splitting by splitting, the transverse phase space for radiation, and the perturbative QCD evolution terminates once the parton virtuality reaches the value  $Q_0 = 1$  GeV, followed by the hadronization using the Lund model [25].

The YAJEM scenario (i) makes the assumption that the virtuality of partons traversing the medium grows according to the medium transport coefficient  $\hat{q}(\zeta)$  which measures the virtuality transfer per unit pathlength. This coefficient is taken proportional to

$$\hat{q}(\zeta) = K \cdot 2 \cdot \epsilon^{3/4}(\zeta) F(\rho(\zeta), \alpha(\zeta)) \quad (1)$$

with

$$F(\rho(\zeta), \alpha(\zeta)) = \cosh \rho(\zeta) - \sinh \rho(\zeta) \cos \alpha(\zeta),$$

where  $\epsilon$  is the local energy density of the hydrodynamical medium,  $F$  is a hydrodynamical flow correction factor accounting for the Lorentz contraction of the scattering centers density as seen by the hard parton for  $\rho(\zeta)$ , which is the local flow rapidity and  $\alpha(\zeta)$ , the angle between the hydrodynamical flow and the parton propagation direction.

For a shower parton  $a$ , created at a time  $\tau_a^0$  and evolving during  $\tau_a$  before branching into a pair of offspring partons, the integrated virtuality as propagated inside the shower code is given by

$$\Delta Q^2 = \int_{\tau_a^0}^{\tau_a^0 + \tau_a} d\zeta \hat{q}(\zeta), \quad (2)$$

which increases the phase space from  $Q^2 \rightarrow Q^2 + \Delta Q^2$  and thereby, the probability for medium-induced radiation. The integration in Eq. (2) is performed over the eikonal trajectory of the parton-initiated shower from the production vertex to the boundary of the medium (see below). Note that this scenario is different from YAJEM-E and the YAJEM-DE [28] [20] where the shower should be evolved down to  $Q_0 = \sqrt{E/L}$  (i.e.  $E$  is the parton's energy and  $L$ , the medium length).

In the second scenario (BW model), the QCD splitting functions are enhanced in the infrared sector according to the form [24],

$$P_{q \rightarrow qg} = \frac{4}{3} \frac{1+z^2}{1-z} \Rightarrow \frac{4}{3} \left( \frac{2(1+f_{\text{med}})}{1-z} - (1+z) \right) \quad (3)$$

This increased branching probability leads to additional medium induced soft gluon production which decreases the jet energy collimation and widens the jet-shape [29, 30], although no explicit flow of momentum between jet and medium is modeled. In particular, from the point of view of the leading parton, this is a fractional energy loss mechanism since it is formulated as a function of the splitting variable  $z$  only: the lost average energy due to the medium effect is proportional to the initial energy of the leading parton. The factor  $f_{\text{med}}$  is assumed to be proportional to

$$f_{\text{med}} = K_f \cdot \int d\zeta [\epsilon(\zeta)]^{3/4} F(\rho(\zeta), \alpha(\zeta)). \quad (4)$$

We will refer to the implementation of the BW prescription for in-medium showers in the following as YA-JEM+BW. This is distinct from the version of the YAJEM code described above, but also from YAJEM-E and YAJEM-DE which are tested against a large body of observables at both RHIC and the LHC (see e.g. Refs. [31–33]).

In a MC treatment of the shower evolution, using a fixed value for  $\Delta Q^2$  or  $f_{\text{med}}$  to characterize the medium is not needed and is in fact not realistic once a comparison with the data is desired. Following the procedure described in Ref. [20], the values of  $\Delta Q^2$  and  $f_{\text{med}}$  for both scenarios are determined event-by-event by embedding the hard process into a hydrodynamical medium [34] starting from a binary vertex at  $(x_0, y_0)$ , and evaluating the line integral in Eq. (2) and Eq. (4) over the eikonal trajectory  $\zeta$  through the medium. Events are then generated for a large number of random  $(x_0, y_0)$  sampled from the transverse overlap profile

$$P(x_0, y_0) = \frac{T_A(\mathbf{r}_0 + \mathbf{b}/2)T_A(\mathbf{r}_0 - \mathbf{b}/2)}{T_{AA}(\mathbf{b})}, \quad (5)$$

where  $T_A$  is a nuclear thickness function  $T_A(\mathbf{r}) = \int dz \rho_A(\mathbf{r}, z)$  obtained from the Woods-Saxon density  $\rho_A(\mathbf{r}, z)$  and  $b$  is the impact parameter. All observables are averaged over a sufficiently large number of events. This procedure leaves two dimensionful parameters  $K$  in Eq. (1) and  $K_f$  in Eq. (4) characterizing the strength of the coupling between parton and medium which are tuned to reproduce the measured nuclear suppression factor  $R_{AA}$  for each scenario in central 200 GeV AuAu collisions (see Ref. [20]).

### 3 Monte Carlo analysis of medium-modified FFs

YAJEM and PYTHIA6 generate back-to-back showers at center-of-mass energy  $\sqrt{s}$ . In order to simulate the huge amount of jets produced in pp (vacuum) and PbPb (medium) in central collisions (10%), we need to compute the initial  $p_T$  distribution of partons before the showering process and its interaction with the medium start (i.e.  $p_T$  stands for the parton transverse momentum and differs from the jet  $P_T$  before clustering and accounting for cuts). In the vacuum, the initial distribution of gluon and quark-initiated showers is determined by the convolution of parton distribution functions (PDFs) and the leading order (LO) matrix elements of the hard scattering cross section at the given factorization scale of the hard process. For the medium, the same calculation is repeated with the nuclear parton distribution functions (nPDFs). PDFs and nPDFs are provided

by the CTEQ [35] and EKS [36] families for pp and PbPb collisions in the vacuum and the medium respectively. In both cases, the initial distribution can be approximated by a fast decreasing power law like  $(1/p_T)^\alpha$ , which is different for RHIC and the LHC.

Since partons are copiously produced in the LHC environment at center-of-mass energy 2.76 TeV, we sample the initial distribution of partons described above by randomly selecting two thousand gluon and quark dijets with center-of-mass energy  $\sqrt{s} \sim 2p_T$  as input to PYTHIA6 (vacuum) and YAJEM (medium) over each  $p_T$  range. Jets are clustered by using the anti- $k_t$  algorithm for each  $p_T$  range inside the jet cone of resolution  $R = 0.3$  with charged particles as in the CMS experiment. Note that we purposely use the default algorithm currently used by all LHC experiments. Our motivation to do so relies on the fact that the anti- $k_t$  is the most robust jet reconstruction algorithm for pp and PbPb collisions at the LHC with respect to underlying events and pileup.

Reconstructed jets can be sorted by  $P_T$  ( $P_{T1} > P_{T2} > \dots$ ) for the analysis such that the most hardest one ( $P_{T1}$ ) can be randomly selected from its pair ( $P_{T2}$ ) event-by-event. Since the correlation between initial parton kinematics ( $p_T$ ) and reconstructed jet kinematics ( $P_T$ ) gets increasingly blurred for small reconstruction radii ( $R = 0.3$ ) and soft background removal ( $p_t > 1$  GeV), the transverse momentum  $P_T$  of various jets on each sample can drop below the original  $p_T$  range of the leading parton (i.e.  $p_T < P_T$ ). Since the CMS data for FFs and the PbPb/pp ratio of FFs spans over four jet  $P_T$  ranges:  $100 \leq P_T(\text{GeV}) \leq 120$ ,  $120 \leq P_T(\text{GeV}) \leq 150$ ,  $150 \leq P_T(\text{GeV}) \leq 300$  and  $100 \leq P_T(\text{GeV}) \leq 300$  [9], a second  $P_T$  filtering is required in order to fulfill CMS trigger bias conditions, such that  $P_T \geq 100$  GeV,  $P_T \geq 120$  GeV,  $P_T \geq 150$  GeV and  $P_T \geq 100$  GeV respectively. The requirement imposed by the trigger selection in the analysis is defined as “biased”, while that including jets with all clustered hadrons is called “unbiased”.

For this reason, the fraction of gluon jets in one sample is decreased by the trigger bias from its theoretical (unbiased) value  $f_g^{\text{u,vac}}$  to  $f_g^{\text{b,vac}}$  for biased showers in the vacuum, and from  $f_g^{\text{u,med}}$  to  $f_g^{\text{b,med}}$  for biased showers in the medium. Their values depend weakly on the chosen medium-induced radiation scenario. The values of  $f_g^{\text{u,vac}}$  and  $f_g^{\text{u,med}}$  can be determined from the initial distribution of gluons in each  $P_T$  range, while  $f_g^{\text{b,vac}}$  and  $f_g^{\text{b,med}}$  can be obtained after computing the fraction of gluon jets passing the  $P_T$  trigger selection. For the sake of a realistic comparison with the CMS data, one should evaluate the mixed FFs which are obtained from the linear combinations of gluon and quark FFs:

$$\left(\frac{dN}{d\xi}\right)_{\text{mixed}} = f_g \left(\frac{dN}{d\xi}\right)_g + (1 - f_g) \left(\frac{dN}{d\xi}\right)_q. \quad (6)$$

For the simulation procedure, we perform a double random selection of events over  $p_T$  and  $\Delta Q^2$  ( $f_{\text{med}}$ ) for the first (second) scenario as input to YAJEM (YAJEM+BW) and average over both variables for a large number of events. In the first scenario, the YAJEM code is run by averaging over  $p_T$  and the medium-induced virtuality  $\Delta Q^2$ , which results in  $(\langle P_T^{\text{u}} \rangle, \langle \Delta Q^2 \rangle)$  and in the second one, it is run as YAJEM+BW by averaging over  $p_T$  and  $f_{\text{med}}$ , which results in  $(\langle P_T^{\text{u}} \rangle, \langle f_{\text{med}} \rangle)$ . Such average values are obtained after embedding the hard process in the hydrodynamical medium, as described in section 2. In such a way, the trigger selection can be applied to the jet  $P_T$  and medium parameter simultaneously after clustering, resulting in  $(\langle P_T^{\text{b}} \rangle, \langle \Delta Q^2 \rangle)$  and  $(\langle P_T^{\text{b}} \rangle, \langle f_{\text{med}} \rangle)$  (i.e.  $\langle P_T^{\text{u}} \rangle$  stands for the average  $P_T$  value over all events after clustering and  $\langle P_T^{\text{b}} \rangle$  is the average  $P_T$  of those jets fulfilling the trigger bias selection.)

### 3.1 Medium-modified FFs and ratio: Comparison with CMS data at 2.76 TeV

In this subsection we proceed to compare the CMS PbPb, pp FFs and the ratio PbPb/pp of FFs with YAJEM, PYTHIA6 and YAJEM/PYTHIA6 versus YAJEM+BW/PYTHIA6 respectively. We note that since the FFs written as a function of  $\xi \equiv \ln(1/z)$  (i.e  $z = p_t/p_T$ ) follow a hump-backed plateau shape, such a shape can be parametrized, without any loss of generality, as a distorted Gaussian (DG) which depends on the original  $p_T$  of the parton in the range  $0 \leq \xi \leq Y$  with  $Y = \ln(p_T/Q_0)$ , evolved down to a shower cut-off scale  $\lambda = \ln(Q_0/\Lambda_{\text{QCD}})$ :

$$D(\xi, Y, \lambda) = \mathcal{N}/(\sigma\sqrt{2\pi}) \cdot e^{\left[\frac{1}{8}k - \frac{1}{2}s\delta - \frac{1}{4}(2+k)\delta^2 + \frac{1}{6}s\delta^3 + \frac{1}{24}k\delta^4\right]}, \quad (7)$$

where  $\delta = (\xi - \bar{\xi})/\sigma$ , with moments:  $\mathcal{N}$  (hadron multiplicity inside the jet),  $\bar{\xi}$  (DG peak position),  $\sigma$  (DG width),  $s$  (DG skewness), and  $k$  (DG kurtosis). The energy-evolution of these moments can be analytically calculated at NNLL+NLO\* accuracy and compared to the jet data to extract a very precise value of the strong QCD coupling  $\alpha_s$  [37–39] in elementary  $e^+e^-$  and  $e^-p$  collisions. In a forthcoming work [40], we plan to generalize such an approach to heavy-ion phenomenology in order to extract the medium transport coefficient  $\hat{q}$  and pathlength  $L$ .

In Table 1 we display the gluon fractions of the biased and unbiased showers for each  $p_T$  range, as well as the unbiased  $\langle P_T^u \rangle$  and biased  $\langle P_T^b \rangle$  transverse momenta.

$p_T$ range (GeV)	$\langle P_T^u \rangle$ (GeV)	$\langle P_T^b \rangle$ (GeV)	$f_g^{\text{u,vac}}$	$f_g^{\text{b,vac}}$	$f_g^{\text{u,med}}$	$f_g^{\text{b,med}}$
100-120	44.6	103.0	0.463	$5.2 \times 10^{-4}$	0.330	$1.1 \times 10^{-4}$
120-150	55.9	124.5	0.399	$1.1 \times 10^{-3}$	0.182	$1.3 \times 10^{-4}$
150-300	97.2	173.8	0.376	$5.1 \times 10^{-2}$	0.174	$1.5 \times 10^{-2}$
100-300	85.8	134.6	0.463	0.168	0.330	0.096

Table 1: Recovered jet transverse momentum and gluon fractions inside the jet cone  $R = 0.3$ .

We display in Figs. 1–4 the PbPb and pp FFs, and their ratios, for various jet  $P_T$  ranges at 2.76 TeV comparing the CMS results to the PYTHIA6, YAJEM and YAJEM+BW predictions. In order to highlight the trends of the data in the plots, we fit the pp and PbPb data points to the DG given by Eq.(7) and produce the ratios  $DG_{\text{med}}/DG_{\text{vac}}$ . The FF  $\xi$  interval is determined by  $\langle P_T^b \rangle$  for each  $p_T$  range and turns to be  $0 \leq \xi \lesssim 5$ . However, since YAJEM is known to fail for very soft hadroproduction from 2 GeV, we limit the phenomenological discussion to the region  $0 \leq \xi \lesssim 4.3$ , where results are expected to be robust. We make use of Eq.(6) for mixed samples of gluon and quark jets and take the fractions of gluon jets displayed in Table 1 for the computation. The FFs for the data ranges  $100 \leq P_T(\text{GeV}) \leq 120$  and  $120 \leq P_T(\text{GeV}) \leq 150$  as displayed by Figs. 1 and 2 show an offset in the comparison with the CMS data in both scenarios, although they fall within the range of CMS uncertainties over all of the  $\xi$  interval. However, we can conclude that the first scenario (i) provides a more accurate physical description of the medium-modified FF as confirmed by the ratios in the right panels of Figs. 1 and 2. Indeed, the first scenario (YAJEM) reproduces the right concavity of the ratio for all  $P_T$  ranges, while the trends in the second approach (YAJEM+BW) show the opposite unphysical behavior and should be discarded from the phenomenological discussion hereafter. The best agreement for FFs in the

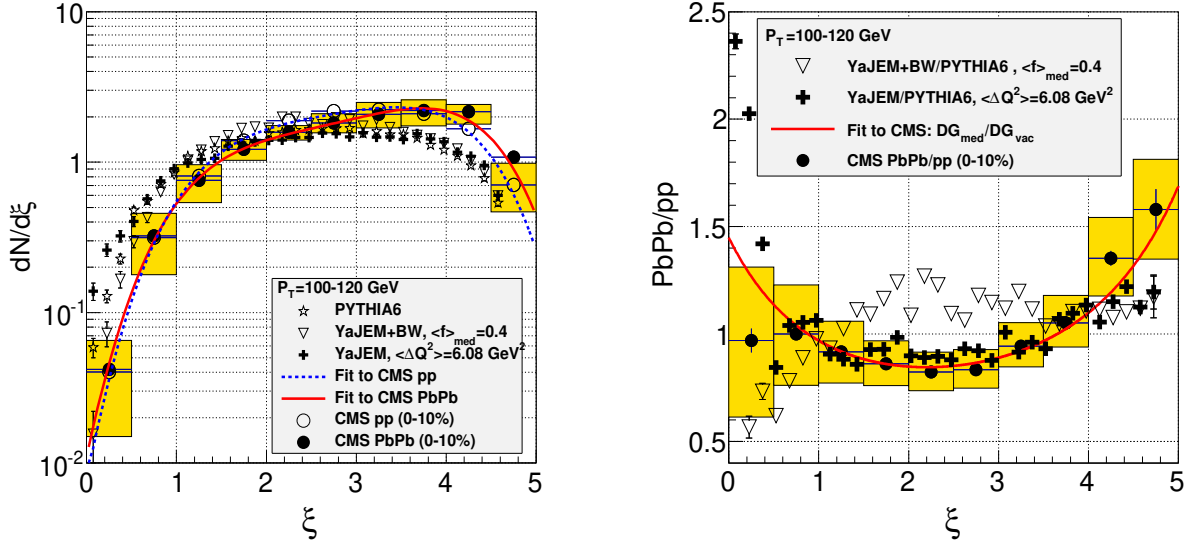


Figure 1: Comparison of jet fragmentation functions in pp and PbPb collisions, for jets with  $100 \leq P_T(\text{GeV}) \leq 120$ , measured by CMS [9] and obtained in two MC approaches (YAJEM and YAJEM+BW): absolute distributions (left), and PbPb/pp ratios (right).

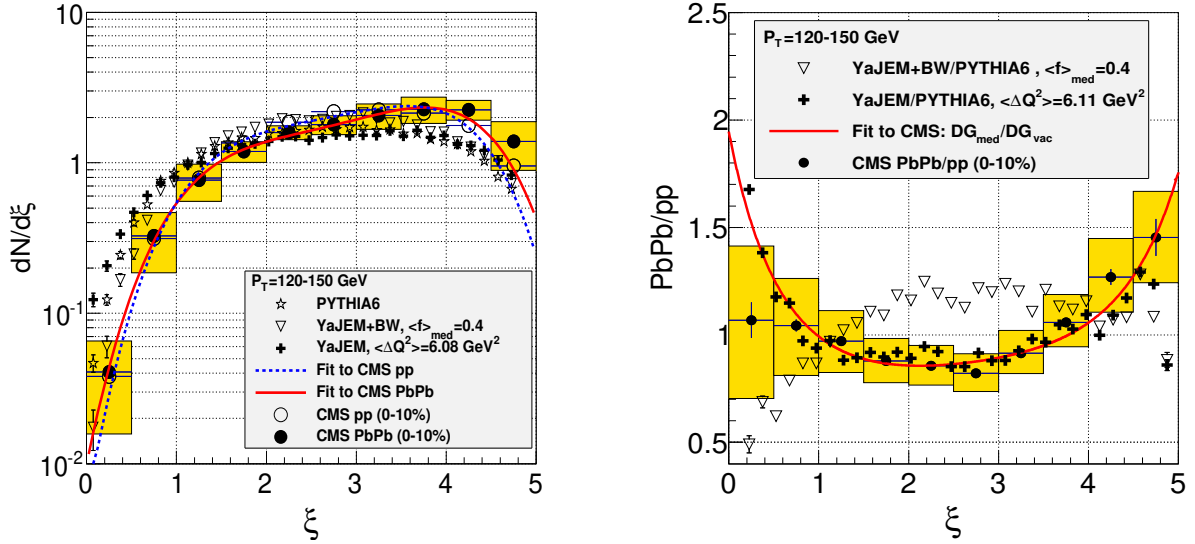


Figure 2: Comparison of jet fragmentation functions in pp and PbPb collisions, for jets with  $120 \leq P_T(\text{GeV}) \leq 150$ , measured by CMS [9] and obtained in two MC approaches (YAJEM and YAJEM+BW): absolute distributions (left), and PbPb/pp ratios (right).

comparison of the CMS data with the MC calculation is reached for the data ranges  $150 \leq P_T(\text{GeV}) \leq 300$  and  $100 \leq P_T(\text{GeV}) \leq 300$  in Figs. 3 and 4 respectively. The first scenario is also here in much better agreement with the CMS PbPb data than that shown by the BW model. Likewise, PYTHIA6 is in good agreement with pp data in both cases. Note that in all panels, we have displayed the averaged values of the hydrodynamical-like parameters  $\Delta Q^2$  and  $f_{\text{med}}$  which turn to be  $\langle \Delta Q^2 \rangle \sim 6 \text{ GeV}^2$  and  $\langle f_{\text{med}} \rangle \sim 0.4$ . For a constant medium of length  $L = 2.5 \text{ fm}$  [41], the transport coefficient would be roughly  $\hat{q} = \langle \Delta Q^2 \rangle / L \sim 2.4 \text{ GeV}^2/\text{fm}$  according to this hydrodynamical prescription of the QGP.

Suppression of the hadron yield in the data is weak and can mainly be observed in the intermediate region around the maximum peak positions of FFs:  $1.0 \lesssim \xi \lesssim 3.6$  ( $0.4 \lesssim z \lesssim 0.7$ ) for all data ranges in the right panels of Figs. 1–4. As a matter of fact, this is not surprising since, being the region where partons fragment more efficiently, they undergo more interactions with the medium and hence, a larger amount of them are dissipated inside the QGP before reaching the hadronization stage. For  $0 < \xi \lesssim 1.0$  ( $1 < z \lesssim 0.4$ ) and  $3.8 \lesssim \xi \lesssim 4.3$  ( $0.7 \lesssim z \lesssim 0.015$ ), hadroproduction is increased in PbPb compared to pp collisions, and particularly by a factor of 3/2 in the softest region  $3.8 \lesssim \xi \lesssim 4.3$ , as expected. However, for the ranges  $100 \leq P_T(\text{GeV}) \leq 120$  and  $120 \leq P_T(\text{GeV}) \leq 150$ , this suppression property has been perfectly described by YAJEM, while for  $150 \leq P_T(\text{GeV}) \leq 300$  and  $100 \leq P_T(\text{GeV}) \leq 300$ , the region of soft hadroproduction is slightly overestimated by YAJEM/PYTHIA6 with a relative error of  $\sim 15\%$ , but still within the CMS data uncertainties.

In Fig. 5, we compare the gluon and quark FFs obtained from PYTHIA6 and YAJEM with the mixed FFs and CMS pp and PbPb data. Gluon jets produce a wider shower broadening than quark jets but they get even more suppressed by reconstruction biases than quark jets, which is clearly shown in Table 1. In both cases, as expected, the quark FFs provided by PYTHIA6 and YAJEM are in better agreement with the data. Similar trends for the ratio were found with an in-medium pathlength  $L$ -evolution as a consequence of gluon decoherence effects (anti-angular ordering) in the QGP [41].

For unbiased showers, the original fraction of gluon jets is relatively higher and should be taken from Table 1 for a direct comparison with biased showers in our MC study. That is why we take the unbiased values for the fractions of gluon jets, recompute Eq. (6) in the given  $P_T$  ranges and display the results in Fig. 6 for  $150 \leq P_T(\text{GeV}) \leq 300$  and  $100 \leq P_T(\text{GeV}) \leq 300$ . As illustrated, the unbiased shower shows an offset in the softest region  $3.5 \lesssim \xi \lesssim 5$  compared to the data and the biased FF simulated with YAJEM. However, this bias is markedly higher for narrower  $P_T$  ranges like  $100 \leq P_T(\text{GeV}) \leq 120$  and  $120 \leq P_T(\text{GeV}) \leq 150$  as displayed in Table 1.

The applicability of the Lund model in this framework relies on the fact that the hadronization of partons takes place in the vacuum. For a specific hadron  $h$  of mass  $m_h$ , the spacial scale at which hadronization takes place is roughly  $\sim E_h/m_h^2$ . For kaons, protons and heavier hadrons this length can be drastically shortened. For pions however, which determine the bulk of the multiplicity distribution in QCD showers, the Lund model can be safely applied such that the essential physical features and trends assumed by YAJEM are still expected to be consistent with the data down to  $\sim 2 \text{ GeV}$ . Its implementation in the PYSHOW algorithm mainly affects the tails of the FFs which in the softest region are widened compared to the parton shower without hadronization, but this effect is equally present in vacuum and medium showers as expected.



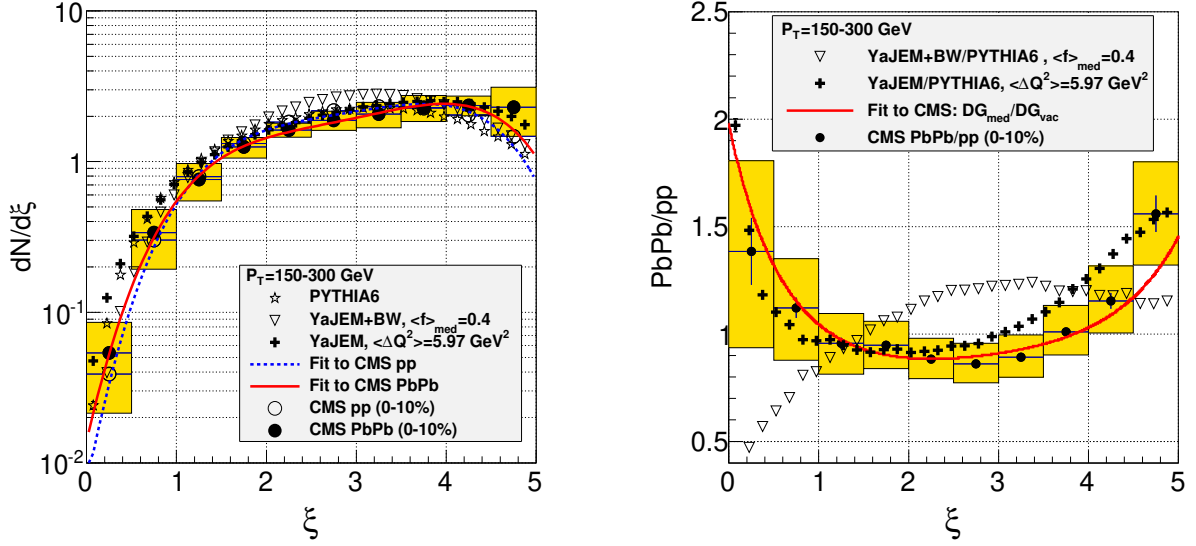


Figure 3: Comparison of jet fragmentation functions in pp and PbPb collisions, for jets with  $150 \leq P_T(\text{GeV}) \leq 300$ , measured by CMS [9] and obtained in two MC approaches (YAJEM and YAJEM+BW): absolute distributions (left), and PbPb/pp ratios (right).

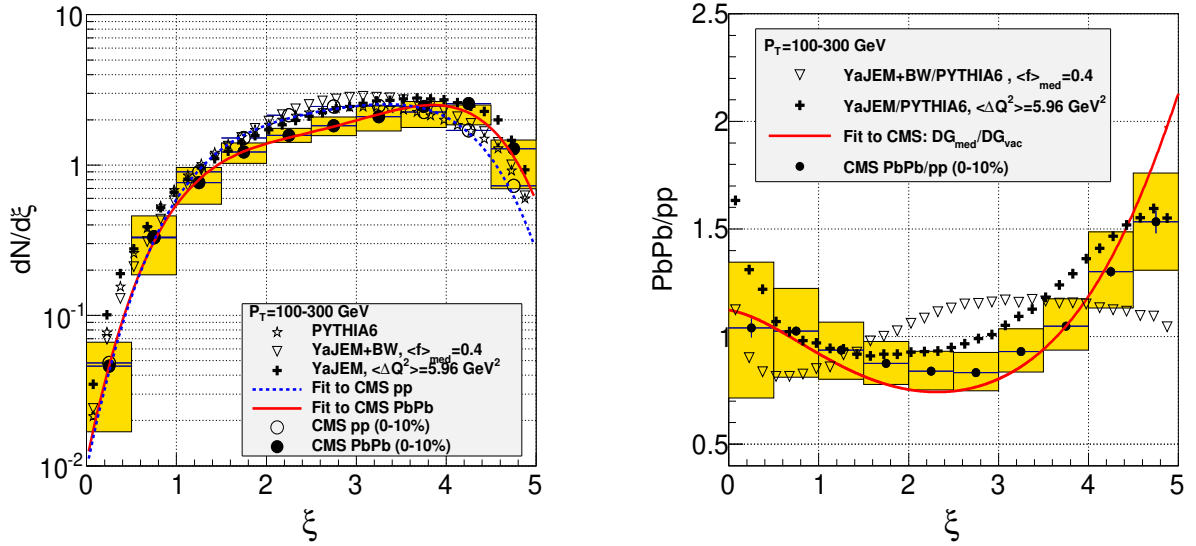


Figure 4: Comparison of jet fragmentation functions in pp and PbPb collisions, for jets with  $100 \leq P_T(\text{GeV}) \leq 300$ , measured by CMS [9] and obtained in two MC approaches (YAJEM and YAJEM+BW): absolute distributions (left), and PbPb/pp ratios (right).

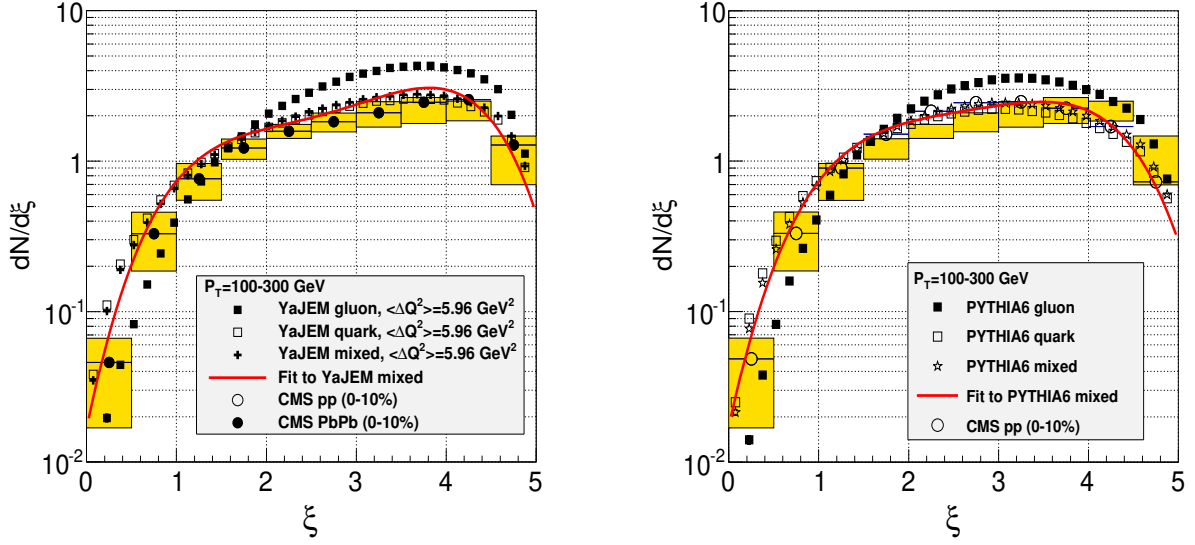


Figure 5: Quark, gluon and parton fragmentation functions in PbPb (left) and pp (right) collisions obtained in the YAJEM MC, for jets with  $100 \leq P_T(\text{GeV}) \leq 300$ , compared to CMS inclusive jet results [9].

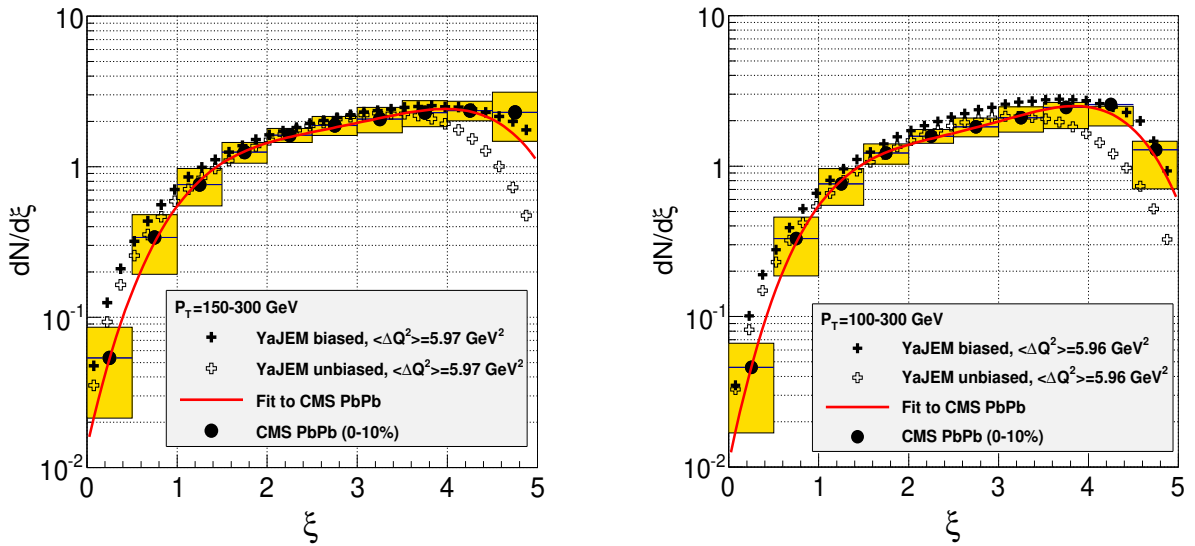


Figure 6: Parton fragmentation functions in PbPb collisions in the YAJEM Monte Carlo, for jets with  $150 \leq P_T(\text{GeV}) \leq 300$  (left) and  $100 \leq P_T(\text{GeV}) \leq 300$  (right) reconstructed applying the data-based cuts (“biased”) or not (“unbiased”), compared to CMS inclusive jet results [9].

## 4 Summary

In this paper, we studied the jet fragmentation functions (FFs) in pp and PbPb collisions, and their ratio, in two different Monte Carlo implementations of parton evolution in a quark-gluon plasma, compared with recent CMS PbPb and pp data at 2.76 TeV. The account of the medium-induced virtuality by the transport coefficient  $\hat{q}$  (YAJEM) is physically successful compared to the BW model (YAJEM+BW) at describing the CMS data and provides a mean  $\hat{q} \sim 2.4 \text{ GeV}^2/\text{fm}$  with  $\Delta Q^2 \sim 6 \text{ GeV}^2$  for a medium of length  $L = 2.5 \text{ fm}$  in the hydrodynamical description of the QGP. The biased FFs and ratios are mainly dominated by quark-initiated showers and are well described by YAJEM over the  $\xi$  interval for all  $P_T$  ranges of the CMS data. As a consequence of the jet quenching phenomena, a weak suppression of the hadron yield in the intermediate region  $0.4 \lesssim z \lesssim 0.7$  as well as the increase of soft hadrons in the softest region  $0.7 \lesssim z \lesssim 0.015$  are well described by YAJEM. The comparison of the biased versus unbiased FFs shows the importance of an accurate simulation of the jet-finding strategy, which suppresses the relevant physics of the jet quenching and therefore, information is lost concerning the early stage of jet evolution and its interaction with the QGP. Indeed, the trigger bias suppresses the range of possible medium modifications brought by the medium-induced soft gluon radiation [42]. Since these results are model-dependent, further comparison of the data with other energy loss event generators such as JEWEL [18] and Q-PYTHIA [22] are certainly interesting to unravel the details of parton energy loss in QCD matter.

## Acknowledgements

R.P.R. strongly thanks Beomsu Chang, David d’Enterria and Jiri Kral for useful discussions, comments on the manuscript and their expert help in numerical calculations.

## References

- [1] PHENIX, K. Adcox et al., Phys. Rev. Lett. 88 (2002) 022301, nucl-ex/0109003.
- [2] STAR, J. Adams et al., Phys. Rev. Lett. 91 (2003) 172302, nucl-ex/0305015.
- [3] ALICE Collaboration, K. Aamodt et al., Phys.Lett. B696 (2011) 30, 1012.1004.
- [4] CMS Collaboration, S. Chatrchyan et al., Eur.Phys.J. C72 (2012) 1945, 1202.2554.
- [5] ATLAS Collaboration, G. Aad et al., Phys.Rev.Lett. 105 (2010) 252303, 1011.6182.
- [6] CMS Collaboration, S. Chatrchyan et al., Phys.Rev. C84 (2011) 024906, 1102.1957.
- [7] PHENIX, A. Adare et al., Phys.Rev.Lett. 111 (2013) 032301, 1212.3323.
- [8] CMS Collaboration, S. Chatrchyan et al., Phys.Lett. B730 (2014) 243, 1310.0878.
- [9] CMS Collaboration, S. Chatrchyan et al., Phys.Rev. C90 (2014) 024908, 1406.0932.

- [10] Y.L. Dokshitzer et al., Gif-sur-Yvette, France: Ed. Frontières (1991) 274 p. (Basics of); and Rev. Mod. Phys. **60** (1988) 373.
- [11] M. Bengtsson and T. Sjostrand, Phys.Lett. B185 (1987) 435.
- [12] E. Norrbin and T. Sjostrand, Nucl.Phys. B603 (2001) 297, hep-ph/0010012.
- [13] R. Baier, D. Schiff and B.G. Zakharov, Ann. Rev. Nucl. Part. Sci. 50 (2000) 37, hep-ph/0002198.
- [14] C.A. Salgado and U.A. Wiedemann, Phys. Rev. Lett. 89 (2002) 092303, hep-ph/0204221.
- [15] M. Gyulassy, P. Lévai and I. Vitev, Phys. Lett. B538 (2002) 282, nucl-th/0112071.
- [16] E. Wang and X.N. Wang, Phys. Rev. Lett. 89 (2002) 162301, hep-ph/0202105.
- [17] D. d'Enterria, (2009), 0902.2011.
- [18] K. Zapp et al., (2008), 0804.3568.
- [19] T. Renk, Phys.Rev. C78 (2008) 034908, 0806.0305.
- [20] T. Renk, Phys.Rev. C79 (2009) 054906, 0901.2818.
- [21] N. Armesto et al., J. Phys. Conf. Ser. 110 (2008) 032001.
- [22] N. Armesto, L. Cunqueiro and C.A. Salgado, (2009), 0907.1014.
- [23] G. Corcella et al., JHEP 0101 (2001) 010, hep-ph/0011363.
- [24] N. Borghini and U.A. Wiedemann, (2005), hep-ph/0506218.
- [25] B. Andersson et al., Phys. Rept. 97 (1983) 31.
- [26] M. Cacciari, G.P. Salam and G. Soyez, Eur.Phys.J. C72 (2012) 1896, 1111.6097.
- [27] M. Cacciari and G.P. Salam, Phys.Lett. B641 (2006) 57, hep-ph/0512210.
- [28] T. Renk, (2014), 1408.6684.
- [29] R. Perez-Ramos and V. Mathieu, Phys.Lett. B718 (2013) 1421, 1207.2854.
- [30] R. Perez-Ramos and T. Renk, Phys.Rev. D90 (2014) 014018, 1401.5283.
- [31] T. Renk, Phys.Rev. C85 (2012) 044903, 1112.2503.
- [32] T. Renk, Phys.Rev. C86 (2012) 061901, 1204.5572.
- [33] T. Renk, Phys.Rev. C87 (2013) 024905, 1210.1330.
- [34] T. Renk et al., Phys.Rev. C84 (2011) 014906, 1103.5308.
- [35] H.L. Lai et al., Phys.Rev. D82 (2010) 054021, 1004.4624.

- [36] K. Eskola, V. Kolhinen and C. Salgado, *Eur.Phys.J. C*9 (1999) 61, hep-ph/9807297.
- [37] D. d'Enterria and R. Prez-Ramos, (2014), 1410.4818.
- [38] D. d'Enterria, . Perez-Ramos and . Redamy, (2014), 1408.2865.
- [39] R. Perez-Ramos and D. d'Enterria, *JHEP* 1408 (2014) 068, 1310.8534.
- [40] D. d'Enterria and R. Perez-Ramos.
- [41] Y. Mehtar-Tani and K. Tywoniuk, (2014), 1401.8293.
- [42] T. Renk, *Phys.Rev. C*88 (2013) 054902, 1212.0646.